

## CHAPTER V



### STRUCTURAL MODEL

Once the concrete plastic model was setup and verified, finite element analysis was used to perform a parametric study for uniaxial compression tests. This parametric study focused on determining the uniaxial compressive model of concrete cylinders under spiral prestress confinement. A series of variables and parameters were set up to determine the relations of those parameters to the uniaxial compressive strength of concrete cylinders under spiral prestressed confinement. A series of variables and parameters were used in this dissertation and results are presented in this chapter.

#### 5.1 Parametric Study by Finite Element Analysis

The series of variables and parameters were setup based on the assumption of investigating the active confinement effects for spiral prestressed systems. Therefore, those variables and parameters were defined to achieve the effect of the geometry and level of prestressed force as stated below in Table 5.1 and Table 5.2.

Defined:

$D_s$	=	diameter of strand
$D$	=	diameter of cylinder
$n$	=	number of strand
$f_{ps}$	=	prestressing stress
$f'_c$	=	compressive strength of concrete

Table 5.1 Series of variables (unit in kg-cm)

Series	$D_s$	$D$	$n$	$\%f_{ps}$	$f'_c$
1	1.27	50	8	25	300
2	1.27	50	8	25	450
3	1.27	50	8	25	600
4	1.27	50	8	50	300
5	1.27	50	8	50	450
6	1.27	50	8	50	600
7	1.27	50	8	75	300
8	1.27	50	8	75	450
9	1.27	50	8	75	600
10	1.27	50	16	25	300
11	1.27	50	16	25	450
12	1.27	50	16	25	600
13	1.27	50	16	50	300
14	1.27	50	16	50	450
15	1.27	50	16	50	600
16	1.27	50	16	75	300
17	1.27	50	16	75	450
18	1.27	50	16	75	600
19	1.27	50	24	25	300
20	1.27	50	24	25	450
21	1.27	50	24	25	600
22	1.27	50	24	50	300
23	1.27	50	24	50	450
24	1.27	50	24	50	600
25	1.27	50	24	75	300
26	1.27	50	24	75	450
27	1.27	50	24	75	600

28	1.27	100	8	100	300
29	1.27	100	16	50	300
30	1.27	100	16	100	300
31	1.27	100	24	66.67	300
32	1.27	100	24	100	300
33	1.27	100	32	75	300
34	1.27	100	32	75	450
35	1.27	100	32	75	600
36	2.54	50	8	25	300
37	2.54	50	8	50	300
38	2.54	50	8	75	300

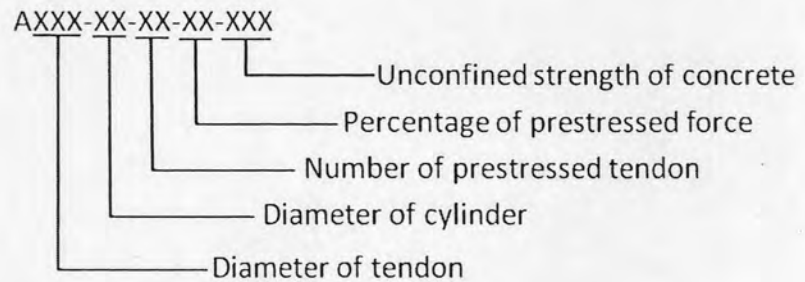
Table 5.2 Series of parameters (unit in kg-cm)

Series	$s$	$f_l$	$s/D$	$f_l/f_c'$	$(P_s/A_g)/f_c'$
1	27.77	6.7	0.56	0.022	0.045
2	27.77	6.7	0.56	0.015	0.030
3	27.77	6.7	0.56	0.011	0.022
4	27.77	13.5	0.56	0.045	0.090
5	27.77	13.5	0.56	0.030	0.060
6	27.77	13.5	0.56	0.023	0.045
7	27.77	20.2	0.56	0.067	0.135
8	27.77	20.2	0.56	0.045	0.090
9	27.77	20.2	0.56	0.034	0.067
10	13.88	13.5	0.28	0.045	0.090
11	13.88	13.5	0.28	0.030	0.060
12	13.88	13.5	0.28	0.023	0.045
13	13.88	27.0	0.28	0.090	0.180
14	13.88	27.0	0.28	0.060	0.120

15	13.88	27.0	0.28	0.045	0.090
16	13.88	40.5	0.28	0.135	0.270
17	13.88	40.5	0.28	0.090	0.180
18	13.88	40.5	0.28	0.068	0.135
19	9.26	20.2	0.19	0.067	0.135
20	9.26	20.2	0.19	0.045	0.090
21	9.26	20.2	0.19	0.034	0.067
22	9.26	40.5	0.19	0.135	0.270
23	9.26	40.5	0.19	0.090	0.180
24	9.26	40.5	0.19	0.068	0.135
25	9.26	60.7	0.19	0.202	0.405
26	9.26	60.7	0.19	0.135	0.270
27	9.26	60.7	0.19	0.101	0.202
28	55.54	6.7	0.56	0.022	0.045
29	27.77	6.7	0.28	0.022	0.045
30	27.77	13.5	0.28	0.045	0.090
31	18.51	13.5	0.19	0.045	0.090
32	18.51	20.2	0.19	0.067	0.135
33	13.88	20.2	0.14	0.067	0.135
34	13.88	20.2	0.14	0.045	0.090
35	13.88	20.2	0.14	0.034	0.067
36	27.77	6.7	0.56	0.022	0.045
37	27.77	13.5	0.56	0.045	0.090
38	27.77	20.2	0.56	0.067	0.135

Study cases were conducted to obtain stress-strain relations for a material model of spiral prestressed concrete. According to the numerical stability of the solving process, the elastic range of concrete material was set up passing through elastic strain,  $\varepsilon_c^{el} \leq 0.0001$ . Thus, plastic strain,  $\varepsilon_c^{pl}$  was observed from historic field

of analysis and plotted against axial stress component as shown on the left figures of Table 5.2. Combining elastic strain,  $\varepsilon_c^{el}$  with plastic strain,  $\varepsilon_c^{pl}$ , total strain,  $\varepsilon_c$  was exhibited as,  $\varepsilon_c = \varepsilon_c^{el} + \varepsilon_c^{pl}$  and can be plotted as shown on the right figures of Table 5.2. The reference serial name is designated according to the following scheme.



The mathematical stress-strain model for axially loaded concrete cylinders with spiral prestressing confinement is shown in Figure 5.1. The model consists of three regions as illustrated. In the first region, Hognestaad's concrete model is applied as a parabolic function from the origin to the peak strength. The second region is assumed to be horizontal from  $\varepsilon_{cc0}$  to  $\varepsilon_{cc1}$ . In the third region the relationship linearly decreases from  $\varepsilon_{cc1}$  to  $\varepsilon_{ccu}$  with a slope  $Z$ . This mathematical model is used in the finite element analysis to acquire values of five parameters. The acquired data from finite element analysis results are given in Table 5.3. The associated graphs are shown in Figure 5.2.

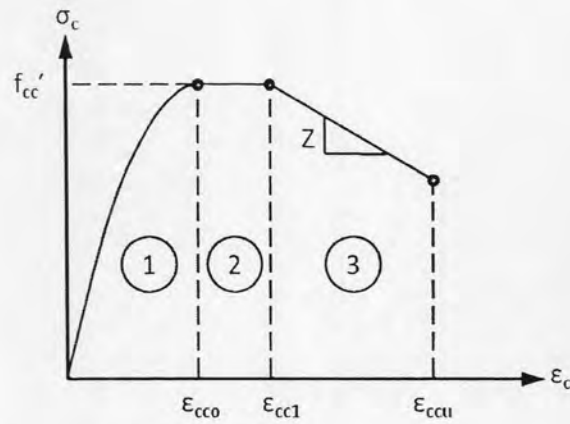


Figure 5.1 Mathematical model for axially loaded concrete cylinder with spiral prestressing confinement

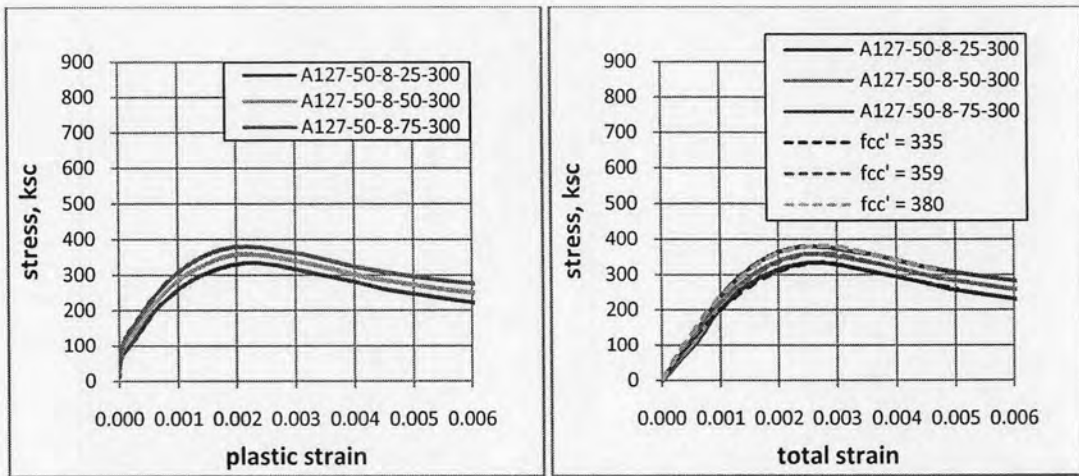


Figure 5.2a Stress-plastic strain relationship and stress-total strain relationship corresponding to assumed function

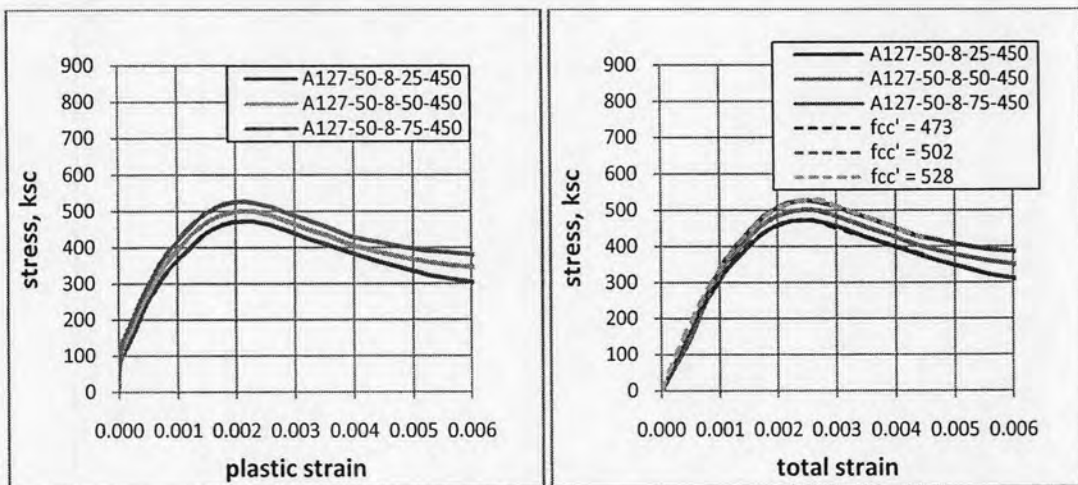


Figure 5.2b Stress-plastic strain relationship and stress-total strain relationship corresponding to assumed function

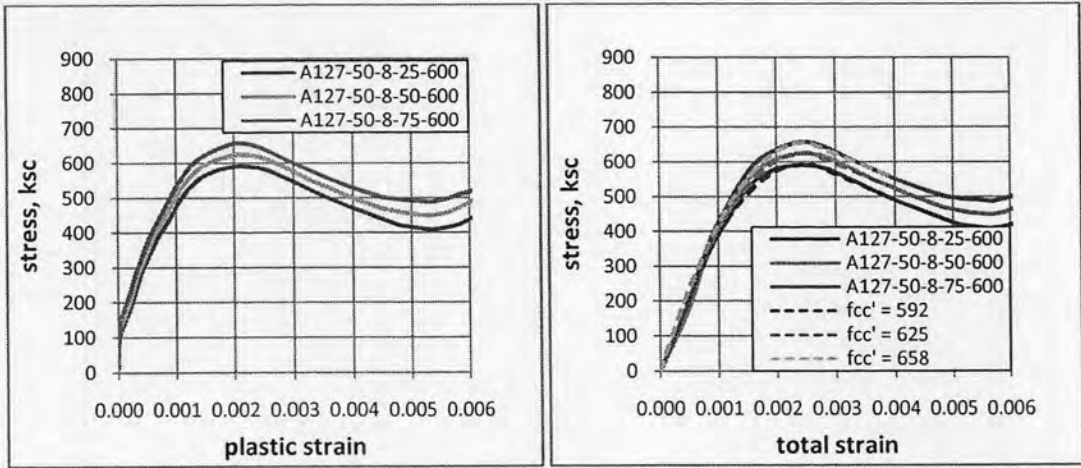


Figure 5.2c Stress-plastic strain relationship and stress-total strain relationship corresponding to assumed function

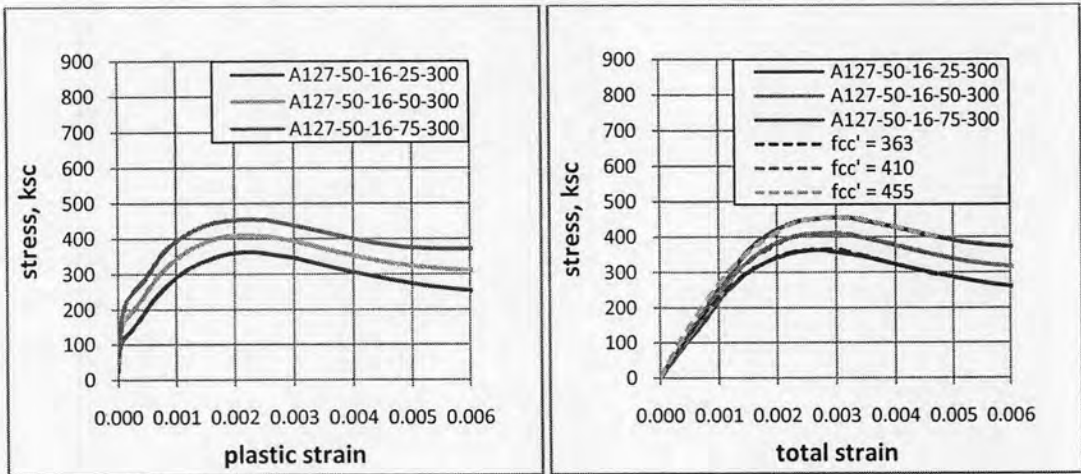


Figure 5.2d Stress-plastic strain relationship and stress-total strain relationship corresponding to assumed function

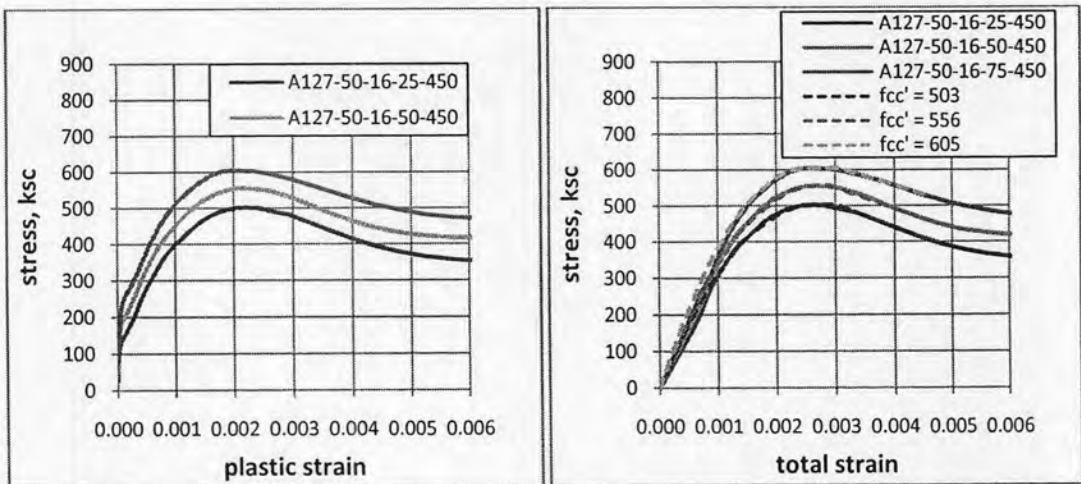


Figure 5.2e Stress-plastic strain relationship and stress-total strain relationship corresponding to assumed function

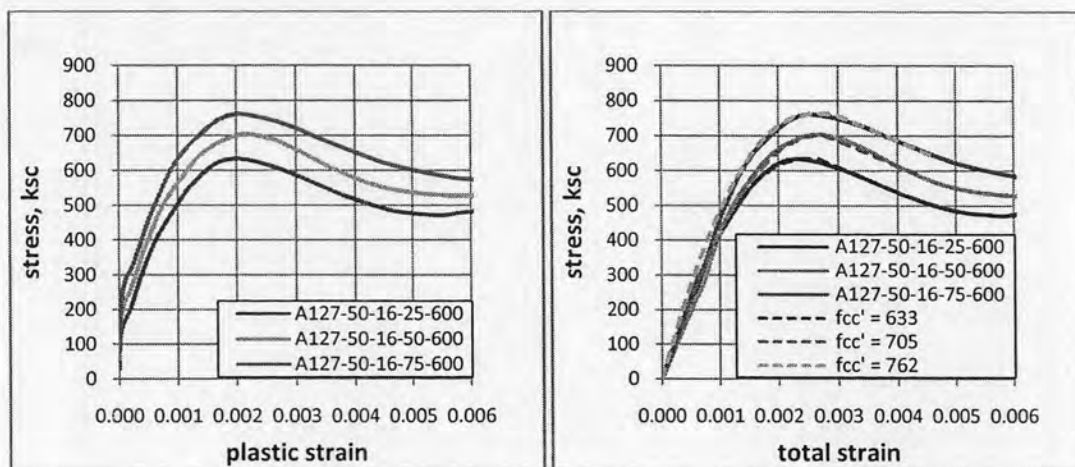


Figure 5.2f Stress-plastic strain relationship and stress-total strain relationship corresponding to assumed function

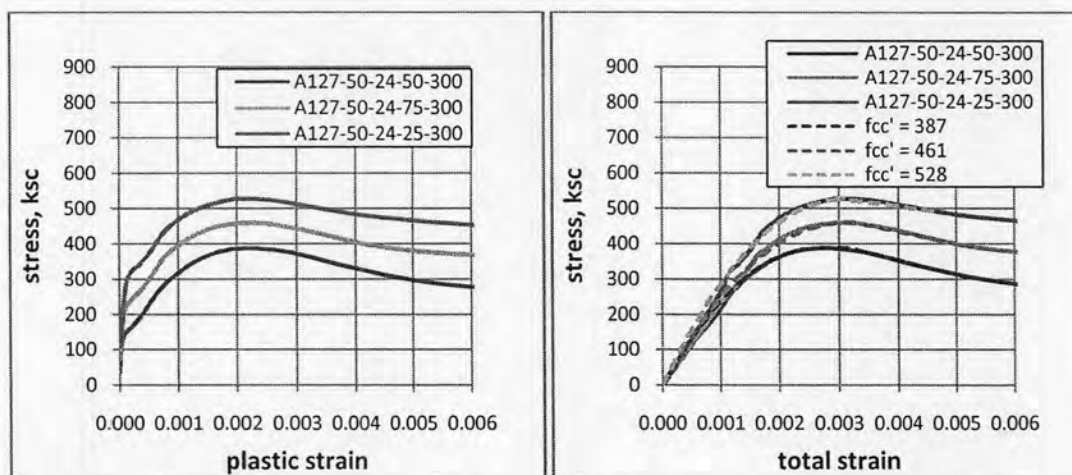


Figure 5.2g Stress-plastic strain relationship and stress-total strain relationship corresponding to assumed function

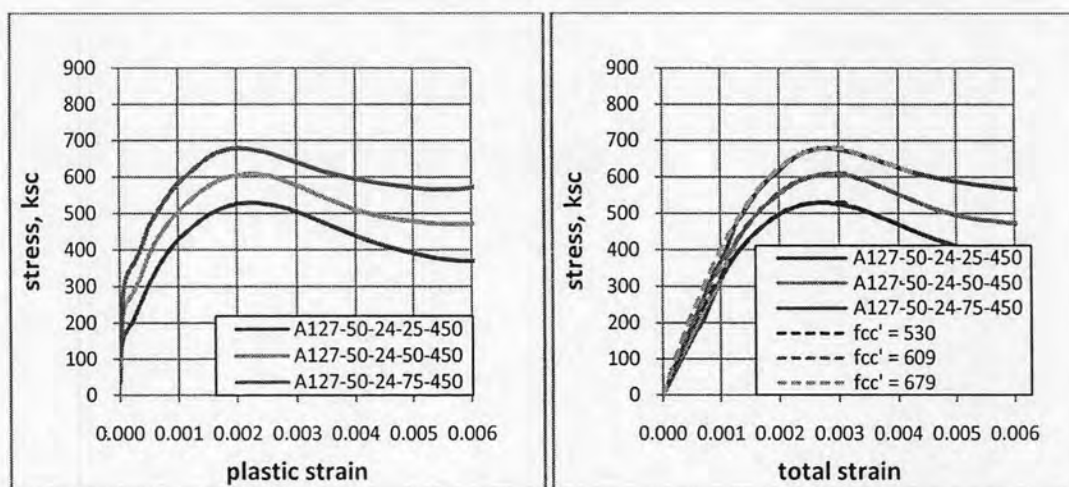


Figure 5.2h Stress-plastic strain relationship and stress-total strain relationship corresponding to assumed function



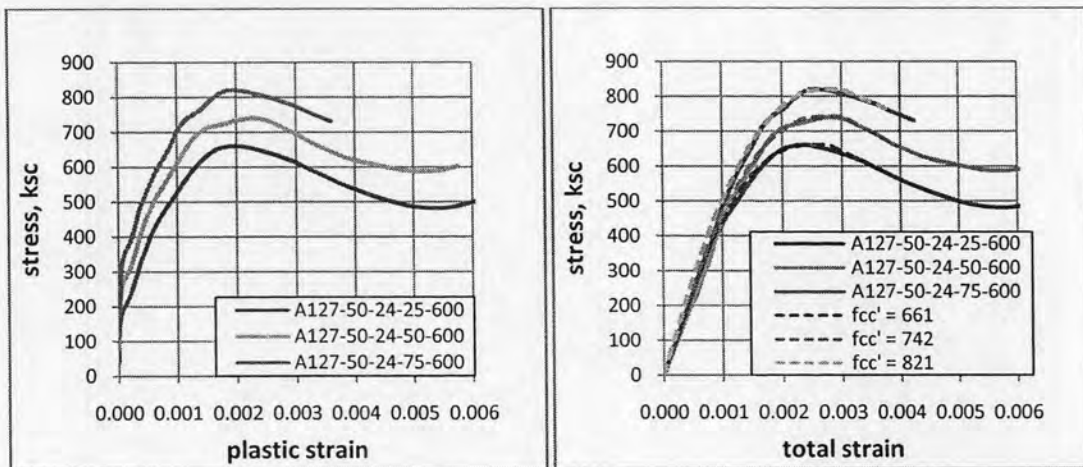


Figure 5.2i Stress-plastic strain relationship and stress-total strain relationship corresponding to assumed function

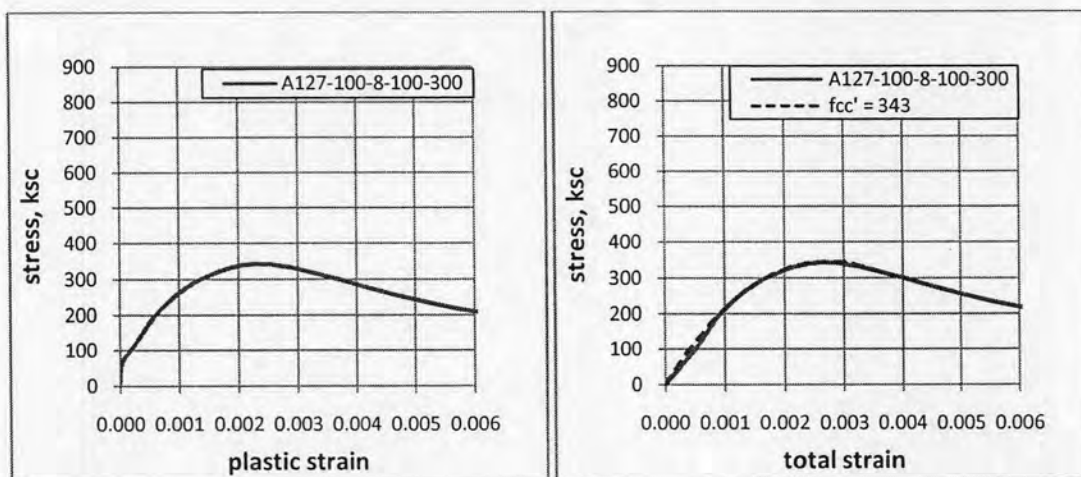


Figure 5.2j Stress-plastic strain relationship and stress-total strain relationship corresponding to assumed function

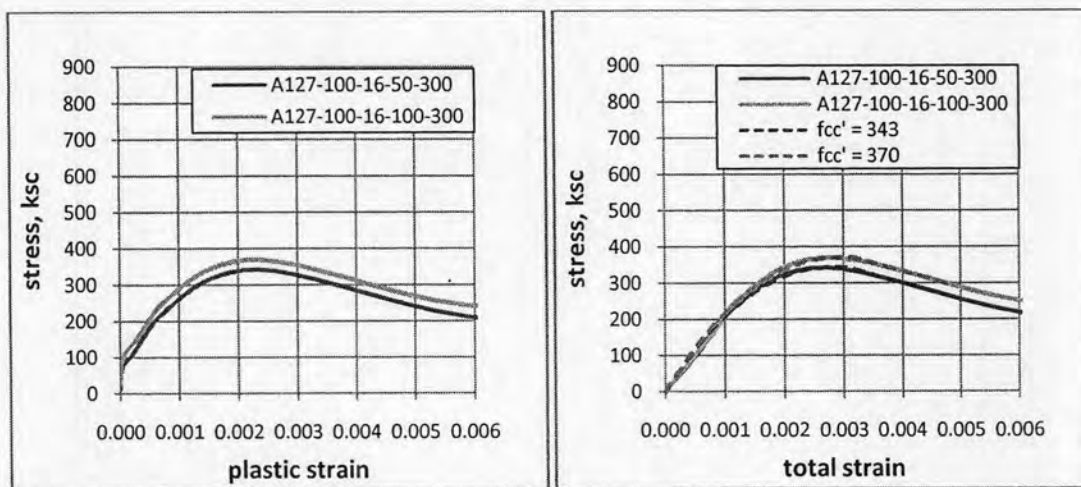


Figure 5.2k Stress-plastic strain relationship and stress-total strain relationship corresponding to assumed function

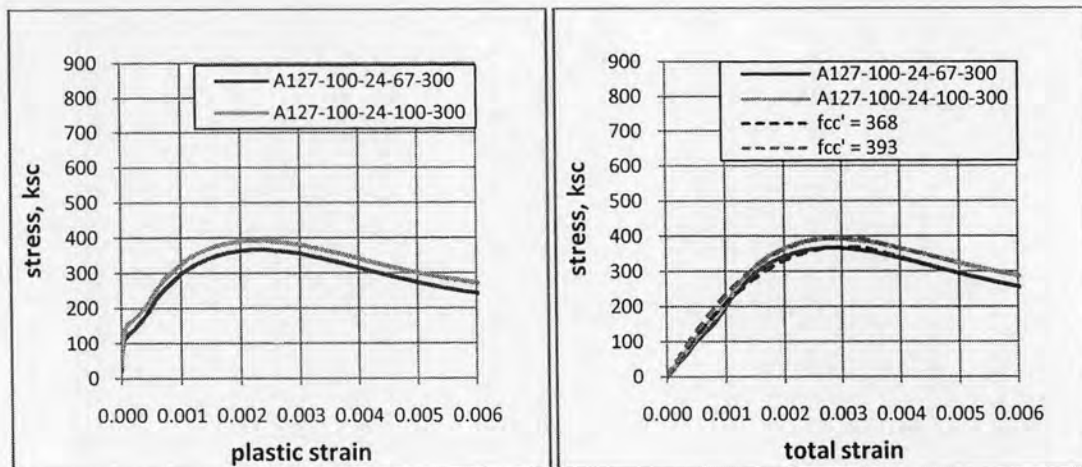


Figure 5.2l Stress-plastic strain relationship and stress-total strain relationship corresponding to assumed function

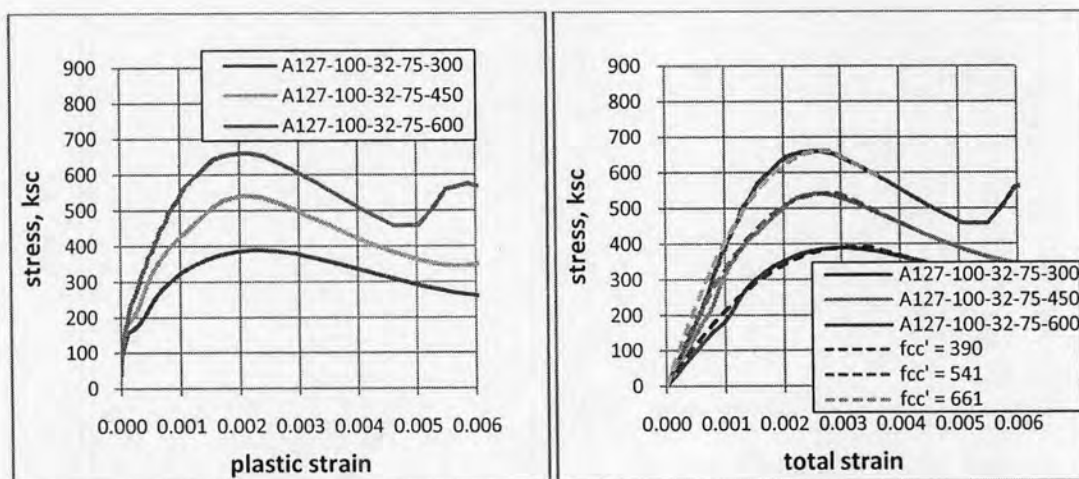


Figure 5.2m Stress-plastic strain relationship and stress-total strain relationship corresponding to assumed function

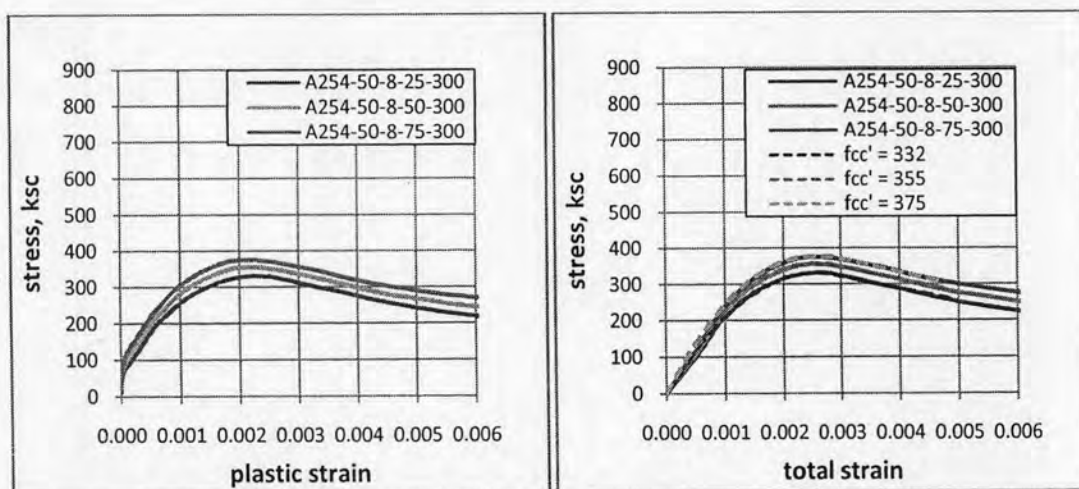


Figure 5.2n Stress-plastic strain relationship and stress-total strain relationship corresponding to assumed function

Table 5.3 Acquired data from finite element analysis results

Series	$k_c$	$\varepsilon_{cco}$	$\varepsilon_{cc1}$	$\varepsilon_{ccu}$	$Z$
1	5.16	0.00274	0.00286	0.00503	34855
2	3.40	0.00241	0.00260	0.00448	51569
3	-1.22	0.00241	0.00263	0.00388	72945
4	4.38	0.00266	0.00299	0.00483	39308
5	3.82	0.00245	0.00268	0.00444	58167
6	1.87	0.00246	0.00257	0.00390	71612
7	3.96	0.00258	0.00301	0.00465	39904
8	3.85	0.00251	0.00274	0.00444	61127
9	2.85	0.00251	0.00251	0.00393	70823
10	4.68	0.00257	0.00308	0.00469	43043
11	3.90	0.00262	0.00302	0.00429	62725
12	2.47	0.00239	0.00268	0.00395	72310
13	4.09	0.00269	0.00318	0.00459	40199
14	3.93	0.00267	0.00291	0.00438	57804
15	3.88	0.00271	0.00274	0.00435	71722
16	3.82	0.00279	0.00333	0.00484	39436
17	3.84	0.00253	0.00306	0.00449	51574
18	4.00	0.00252	0.00293	0.00459	71758
19	4.33	0.00267	0.00317	0.00482	41023
20	3.95	0.00265	0.00308	0.00440	66021
21	3.02	0.00234	0.00278	0.00387	80749
22	3.97	0.00311	0.00325	0.00494	34736
23	3.92	0.00284	0.00312	0.00426	63971
24	3.50	0.00260	0.00302	0.00396	91303
25	3.75	0.00310	0.00300	0.00473	21910
26	3.78	0.00279	0.00306	0.00422	55995
27	3.64	0.00264	0.00301	0.00376	74528

28	6.48	0.00262	0.00305	0.00471	44951
29	6.41	0.00269	0.00305	0.00477	44359
30	5.16	0.00285	0.00317	0.00483	44522
31	5.00	0.00292	0.00338	0.00502	45101
32	4.62	0.00277	0.00333	0.00489	41437
33	4.45	0.00306	0.00352	0.00481	45081
34	4.49	0.00268	0.00298	0.00419	79099
35	3.01	0.00265	0.00284	0.00363	89007
36	4.71	0.00256	0.00272	0.00481	34054
37	4.11	0.00249	0.00279	0.00488	35086
38	3.72	0.00245	0.00288	0.00471	37704

The acquired data will be used to interpret the mathematical stress-strain model for axially loaded concrete cylinders with spiral prestressing confinement considered as a structural model of spirally post-tensioning column.

## 5.2 Proposed Structural Model

All series of parametric studies were used to investigate the structural model of spirally post-tensioned systems. The mathematical model parameters acquired from finite element analysis are  $k_c$ ,  $\varepsilon_{cc0}$ ,  $\varepsilon_{cc1}$ ,  $\varepsilon_{ccu}$  and  $Z$ , as determined in this section.

### *Determination of the relation of $k_c$*

From the investigation,  $k_c$  mainly relates to the active confined pressure,  $f_l$  and strength of concrete,  $f'_c$ . The relation of  $k_c$  to those parameters is shown in Figure 5.3 and Figure 5.4.

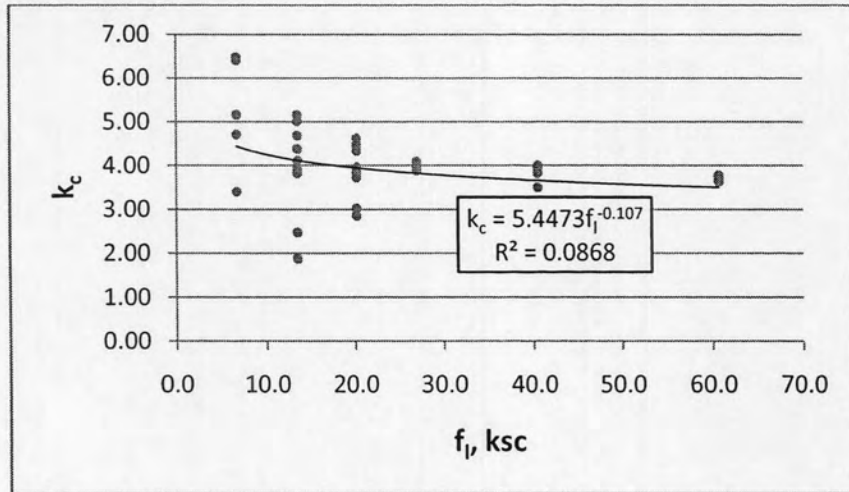


Figure 5.3  $k_c$  vs  $f_l$  relation

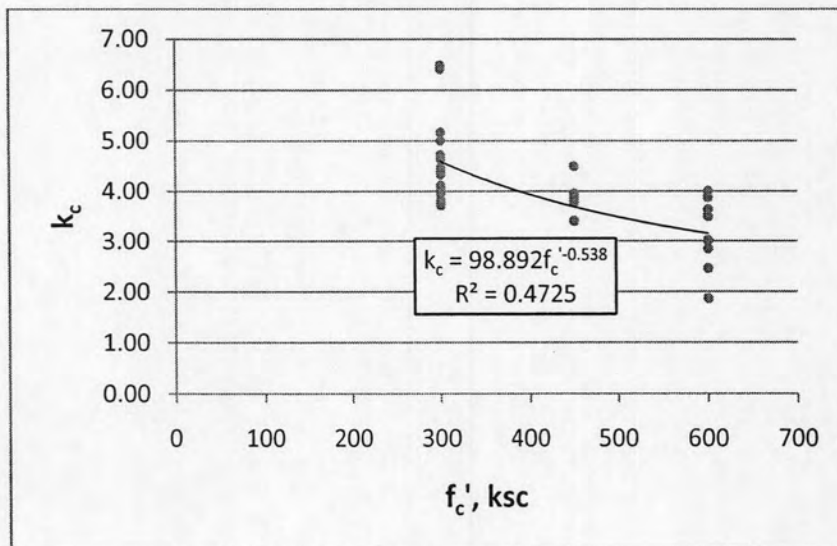


Figure 5.4  $k_c$  vs  $f_c'$  relation

Applying an assumption of the interpolation utilizing a power function, the relation of both parameters can be superimposed and can be plotted as shown in Figure 5.5.

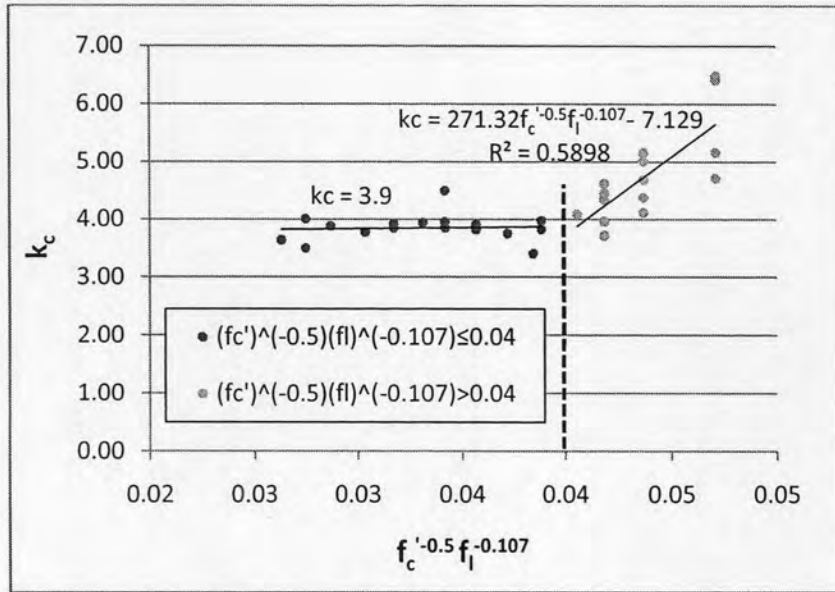


Figure 5.5  $\sqrt{f'_c}^{-1} f_l^{-0.107}$  vs  $k_c$  relation

Referring to Figure 5.5, the relation of  $\sqrt{f'_c}^{-1} f_l^{-0.107}$  and  $k_c$  can be described by a bilinear function. For  $\sqrt{f'_c}^{-1} f_l^{-0.107} \leq 0.04$ ,  $k_c$  tends to be uniformly constant around a value of 3.9. For  $\sqrt{f'_c}^{-1} f_l^{-0.107} > 0.04$ ,  $k_c$  linearly increase with the increasing value of  $\sqrt{f'_c}^{-1} f_l^{-0.107}$ . The relation can be expressed in the formula below,

$$k_c = \begin{cases} 3.9 & \text{for } \sqrt{f'_c}^{-1} f_l^{-0.107} \leq 0.04 \\ 271\sqrt{f'_c}^{-1} f_l^{-0.107} - 7.1 & \text{for } \sqrt{f'_c}^{-1} f_l^{-0.107} > 0.04 \end{cases} \quad (5.1)$$

Plotting the relation of  $\sqrt{f'_c}^{-1} f_l^{-0.107}$  and  $k_c$  corresponding to  $s/D$  ratio as shown in Figure 5.6, all values are closely represented by the proposed function except for those values corresponding to  $s/D = 0.56$ . The values of  $k_c$  corresponding to  $s/D = 0.56$  decreasingly deviate from the lower values of  $s/D$  ratios. According to the study of Shamim A. Sheikh and Murat T. Toklucu (1993), spiral stirrup steel of concrete column could reach the maximum confined concrete strength if  $s/D$  ratios are not greater than 0.36. For a highly confined column,  $s/D$  ratios should not exceed 0.24.

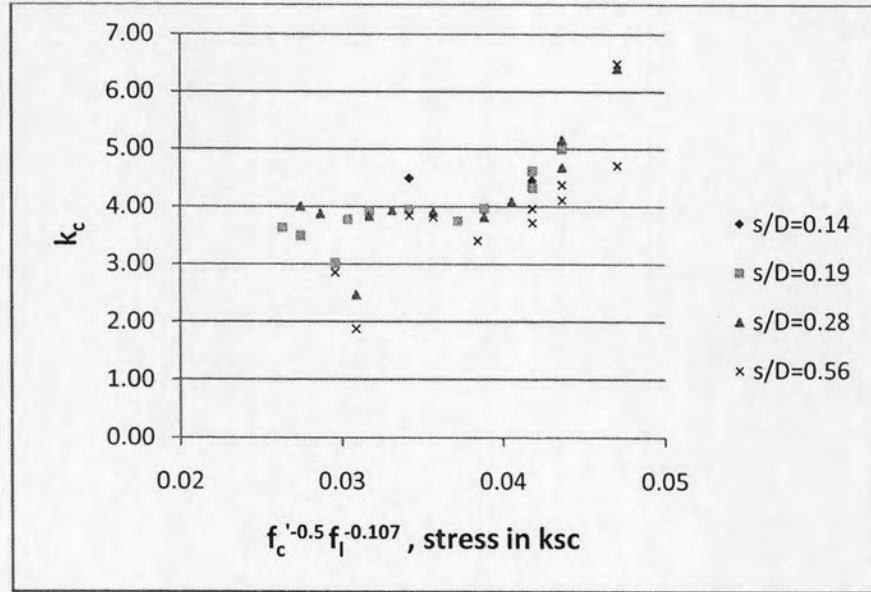


Figure 5.6  $\sqrt{f_c'}^{-1} f_l^{-0.107}$  vs  $k_c$  relation corresponding to  $s/D$  ratios

**Determination of the relation of  $\epsilon_{cco}$**

From the study of Kent and Park (1971) and Sheikh et al. (1986),  $\epsilon_{cco}$  is proportional to  $f_{cc}'/f_c'$ . Plotting  $\epsilon_{cco}$  against  $f_{cc}'/f_c'$ , the relationship of those parameters is shown in Figure 5.7.

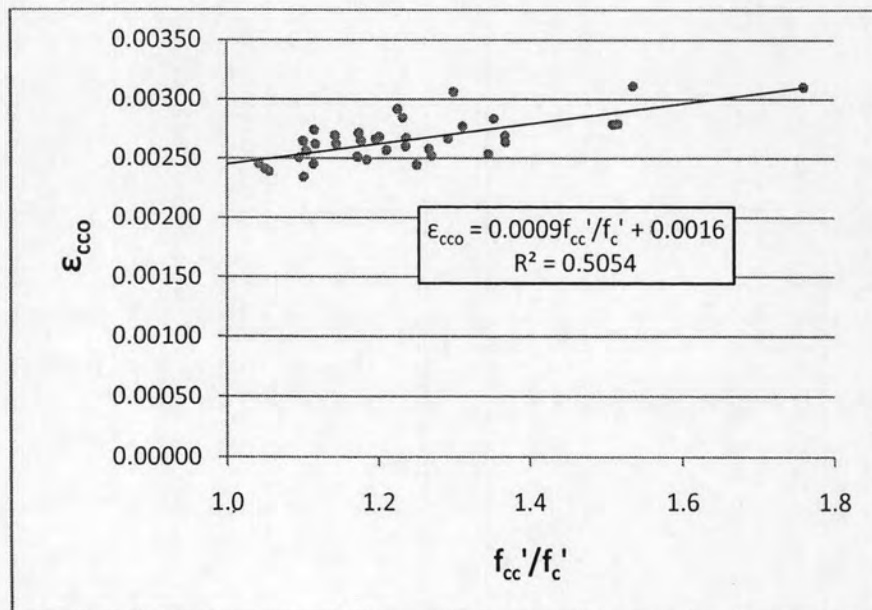


Figure 5.7  $\epsilon_{cco}$  vs  $f_{cc}'/f_c'$  relation

The parameter,  $\varepsilon_{cco}$  under a spiral post-tensioning system can be expressed as:

$$\varepsilon_{cco} = 0.0009 f'_{cc}/f'_c + 0.0016 \quad (5.2)$$

#### **Determination of the relation of $\varepsilon_{cc1}$**

$\varepsilon_{cc1}$  was assumed to extend the stress-strain relation from strain corresponding to the ultimate strength,  $\varepsilon_{cco}$  to the linearly descending portion as shown in Figure 5.1. By investigation,  $\varepsilon_{cc1}$  is proportional to  $f'_{cc}/f'_c$  and can be plotted as shown in Figure 5.8.

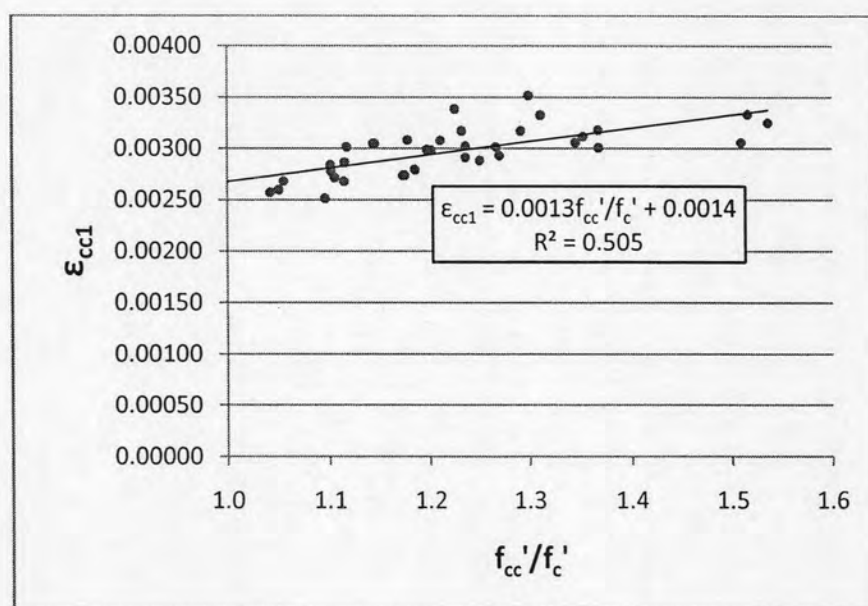


Figure 5.8  $\varepsilon_{cc1}$  vs  $f'_{cc}/f'_c$  relation

The parameter,  $\varepsilon_{cc1}$  under a spiral post-tensioning system can be expressed as:

$$\varepsilon_{cc1} = 0.0013 f'_{cc}/f'_c + 0.0014 \quad (5.3)$$

#### **Determination of the relation of $\varepsilon_{ccu}$**

According to the assumption of Kent and Park (1971) and Sheikh et al. (1986),  $\varepsilon_{ccu}$  is proportional to  $f'_{cc}$ . Plotting  $\varepsilon_{cco}$  against  $f'_{cc}$ , the relationship of those parameters is shown in Figure 5.9.



Under the theory of plasticity through finite element analysis, the investigation of this dissertation shows that the ultimate strain,  $\epsilon_{ccu}$  is proportional to axial compressive strength of concrete,  $f'_c$  as shown in Figure 5.10.

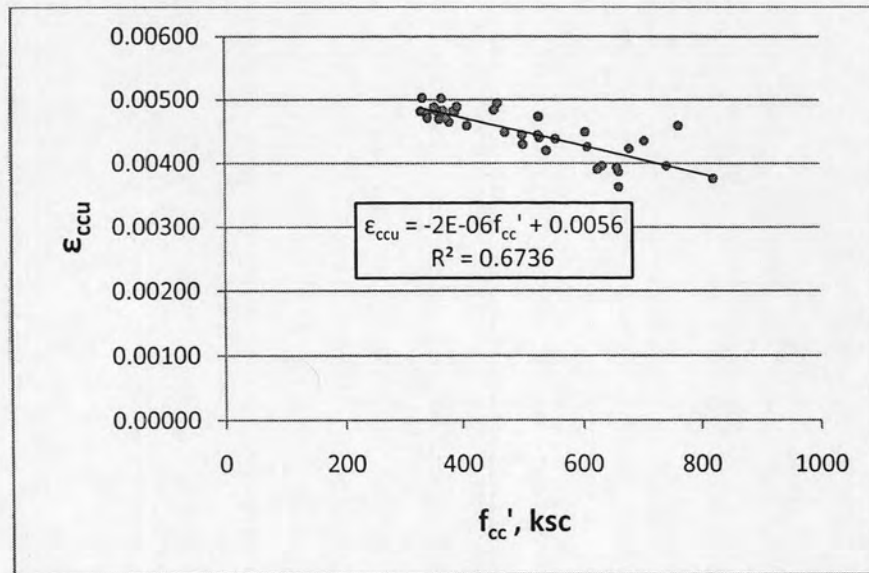


Figure 5.9  $\epsilon_{ccu}$  vs  $f'_{cc}$  relation

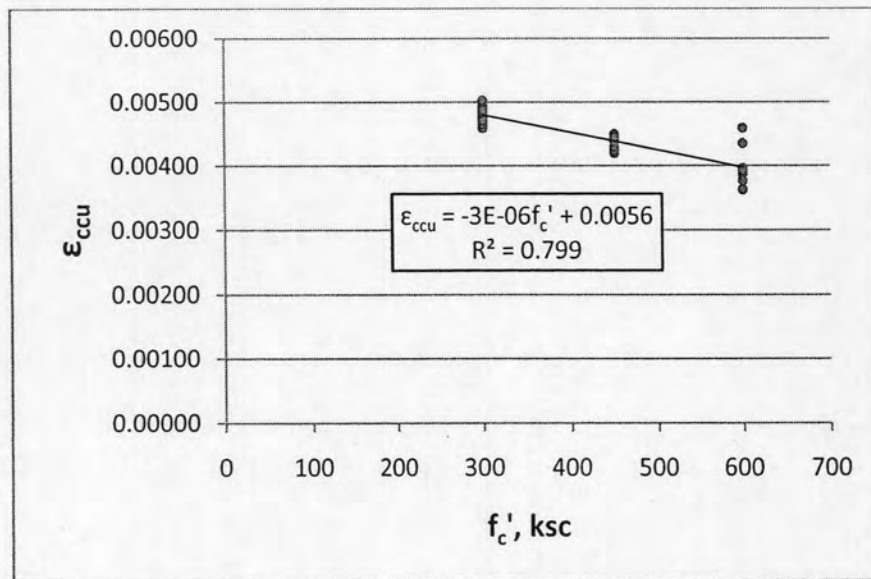


Figure 5.10  $\epsilon_{ccu}$  vs  $f'_c$  relation

The proposed formula for the ultimate strain,  $\epsilon_{ccu}$  can be expressed as:

$$\epsilon_{ccu} = -3 \times 10^{-6} f'_c + 0.0056 \quad (5.4)$$

**Determine the relation of  $Z$**

The descending portion from  $\varepsilon_{cc1}$  to  $\varepsilon_{ccu}$  decreases with slope of  $Z$ . The parameter  $Z$  is proportional to  $f'_c$  and can be plotted as shown in Figure 5.11.

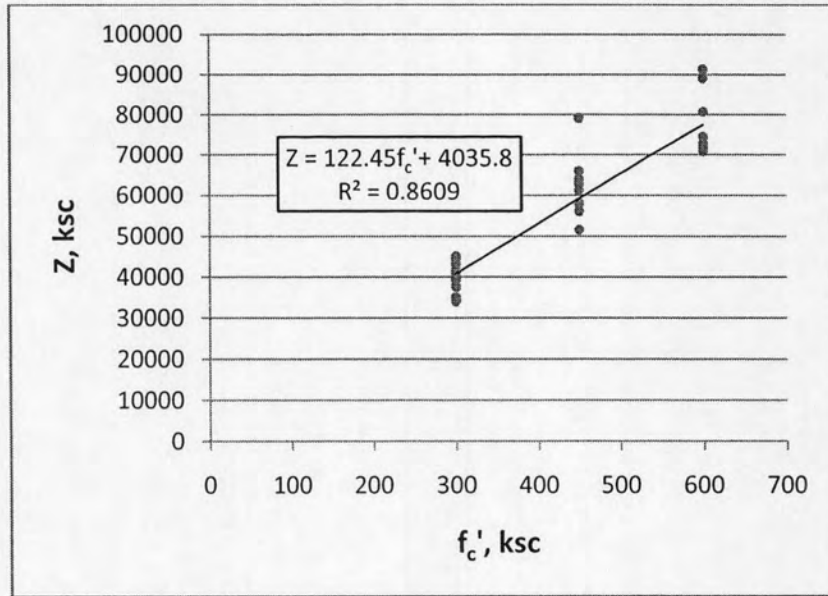


Figure 5.11  $Z$  vs  $f'_c$  relation

The proposed formula for the descending slope,  $Z$  can be expressed as:

$$Z = 122.45f'_c + 4036 \quad (5.4)$$

This parametric study also provided three series to investigate the effect of tendon diameter,  $D_s$ . The results are plotted as shown in Figure 5.12 to evaluate the variable effect of tendon diameter,  $D_s$ .

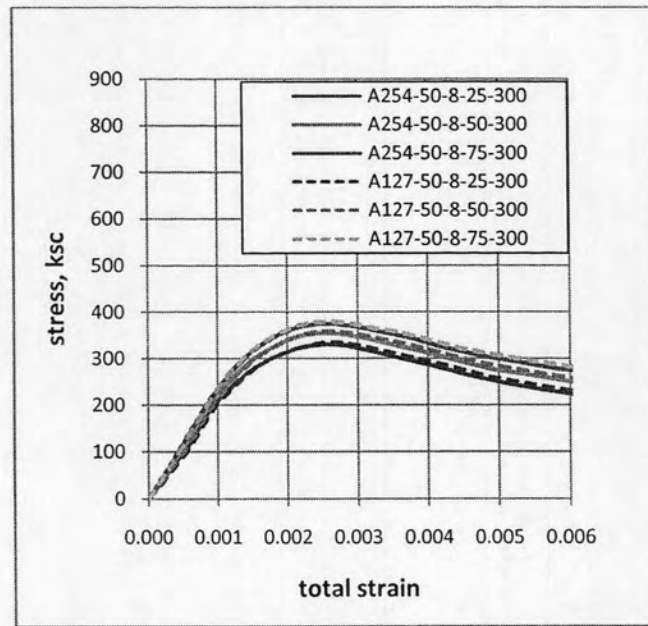


Figure 5.12 Stress - total strain relationship corresponding to the effect of tendon diameter,  $D_s$

Referring to Figure 5.12, the results are not widely separated indicating that tendon diameter,  $D_s$  is not significant as long as the prestressing force from the tendon can be transferred to the concrete without causing local failure.

From the proposed structural model of spiral post-tensioning system, the proposed model is plotted to compare with the finite element analysis results as shown in Figure 5.13.

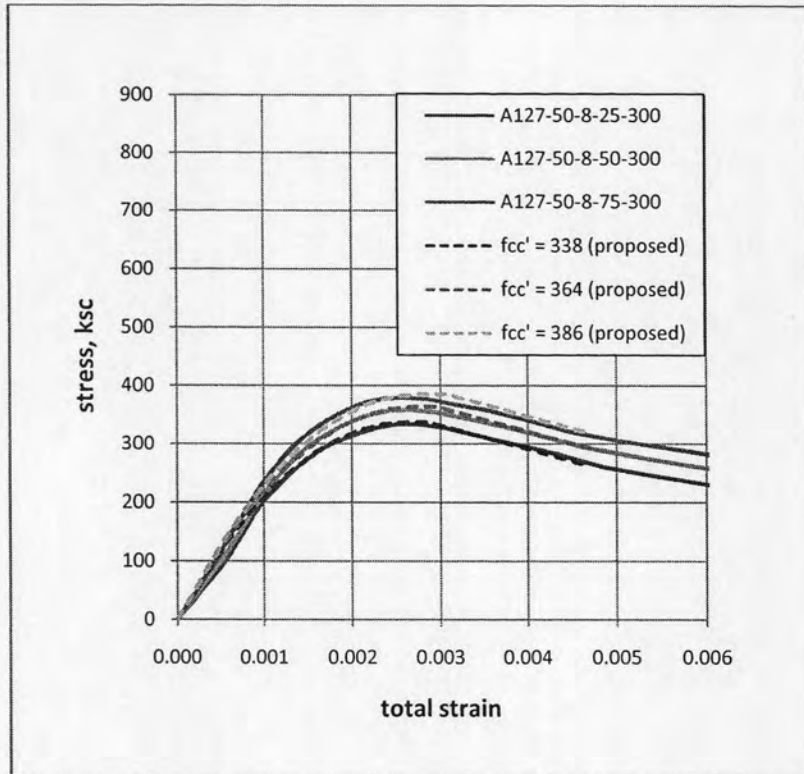


Figure 5.13a Stress – total strain relationship, comparison with the proposed model

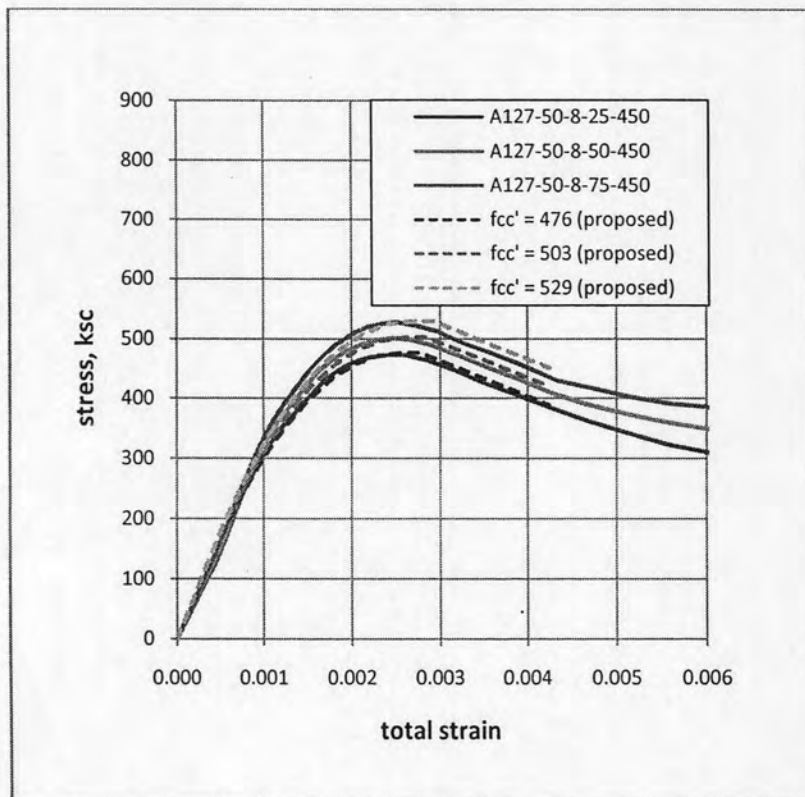


Figure 5.13b Stress – total strain relationship, comparison with the proposed model

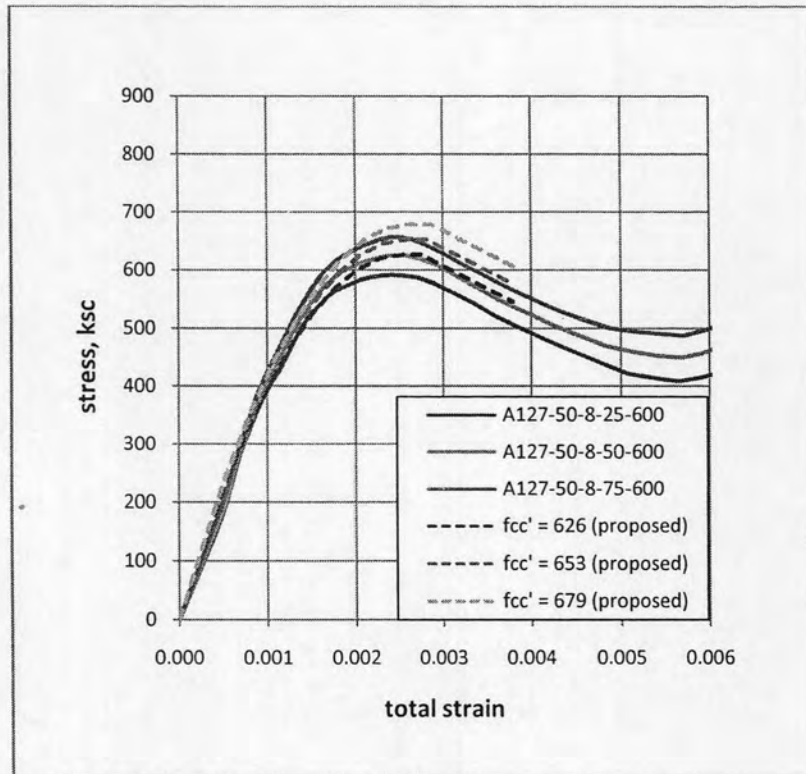


Figure 5.13c Stress – total strain relationship, comparison with the proposed model

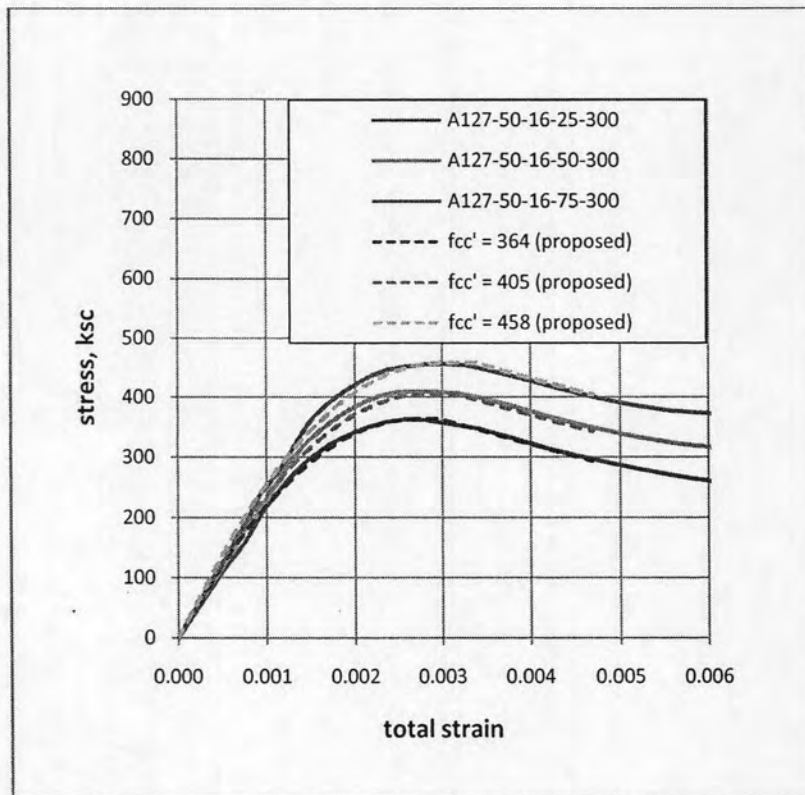


Figure 5.13d Stress – total strain relationship, comparison with the proposed model

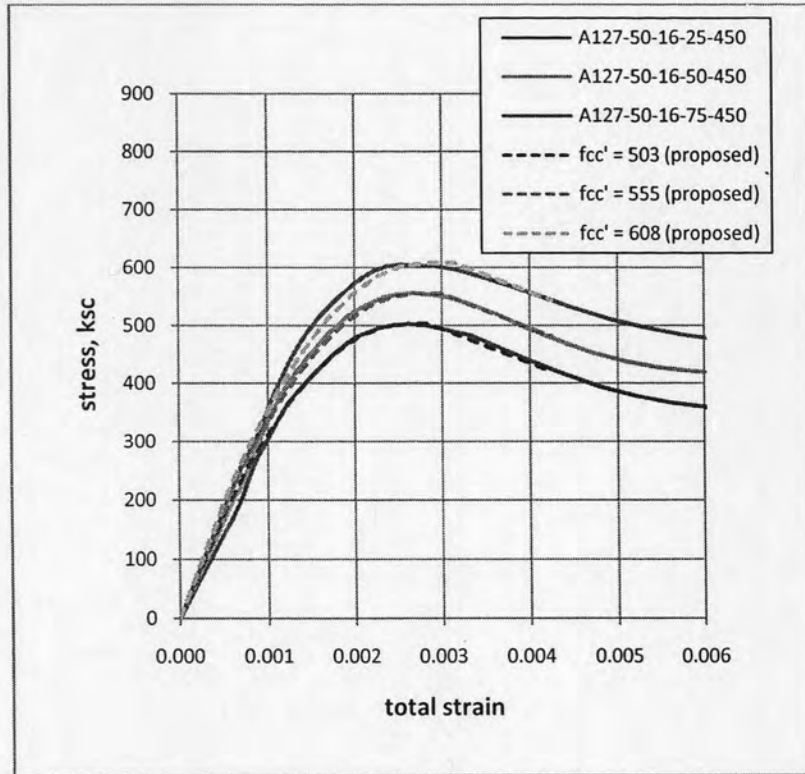


Figure 5.13e Stress – total strain relationship, comparison with the proposed model

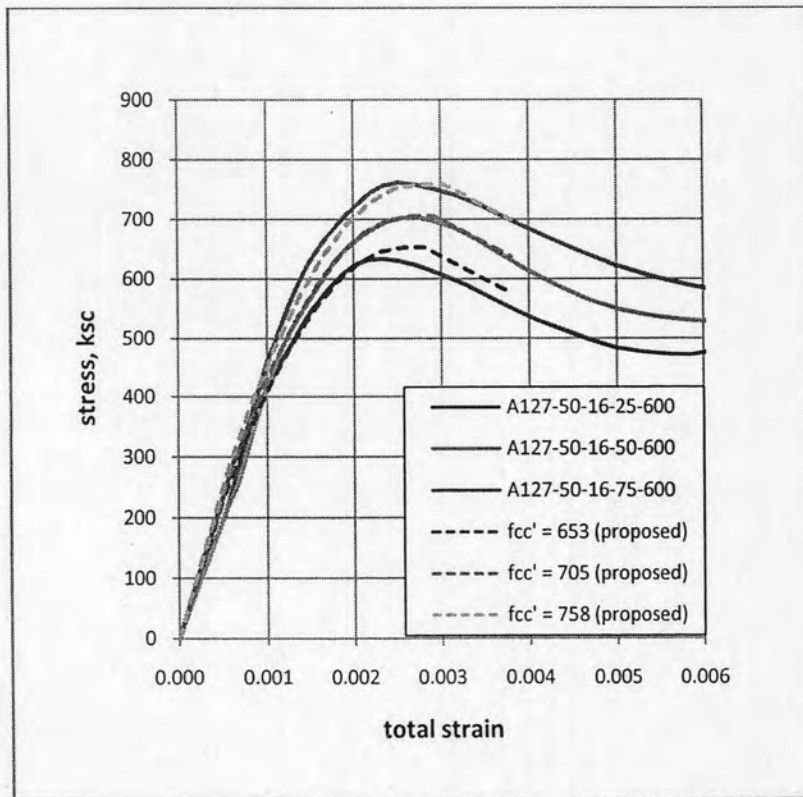


Figure 5.13f Stress – total strain relationship, comparison with the proposed model

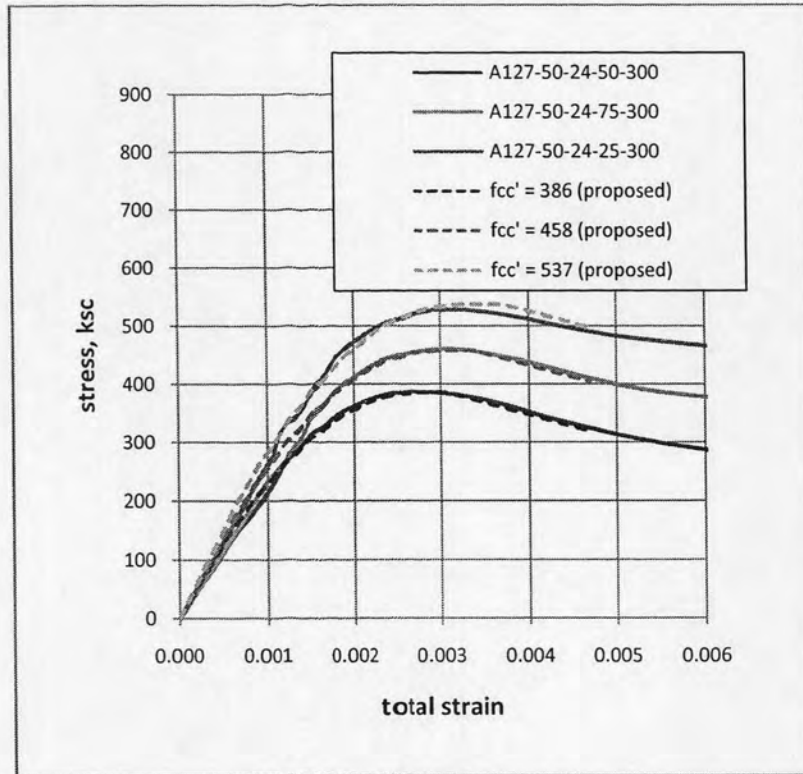


Figure 5.13g Stress – total strain relationship, comparison with the proposed model

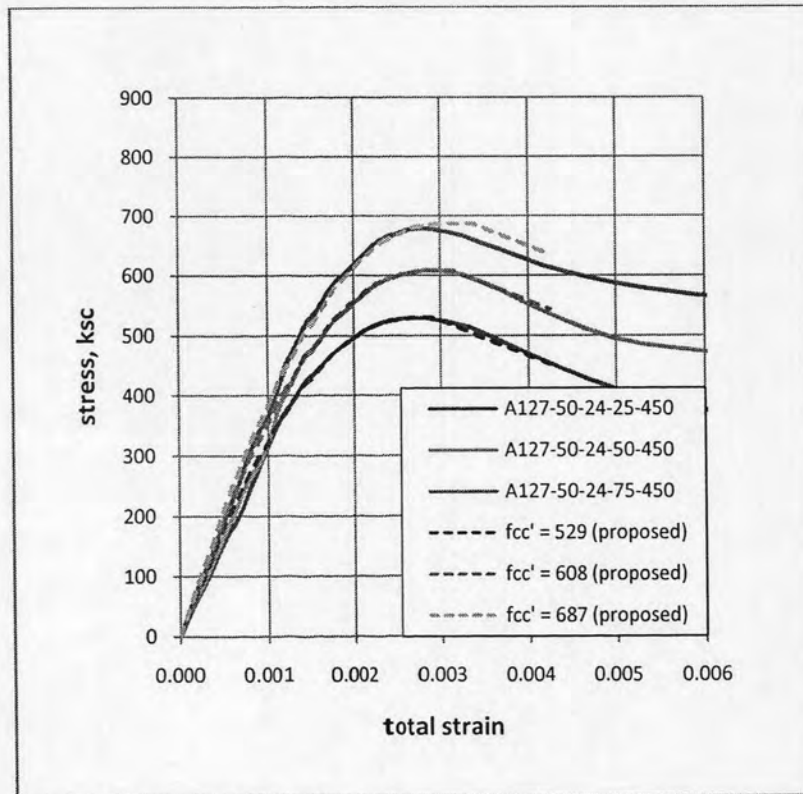


Figure 5.13h Stress – total strain relationship, comparison with the proposed model

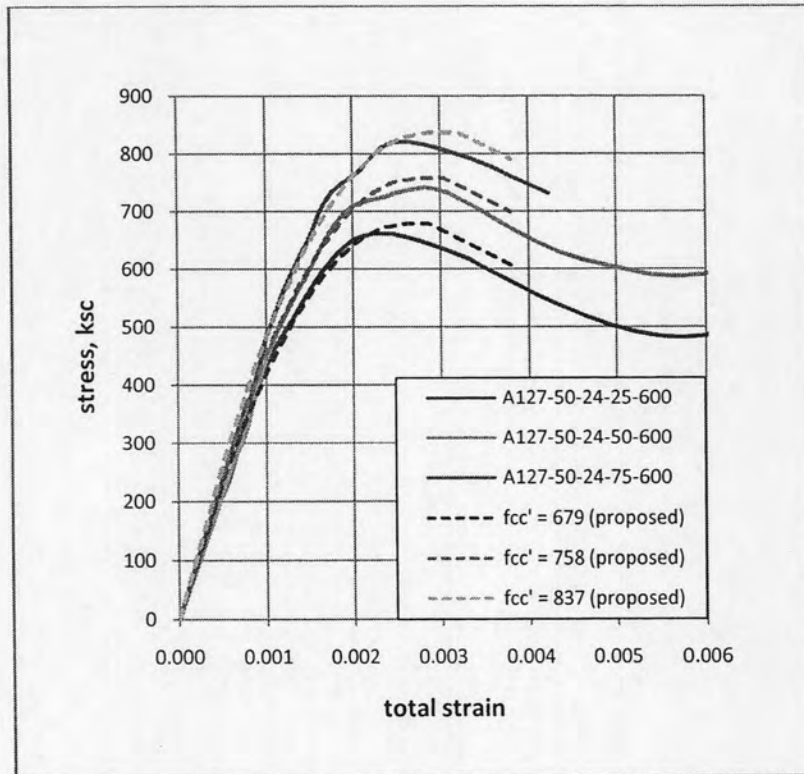


Figure 5.13i Stress – total strain relationship, comparison with the proposed model

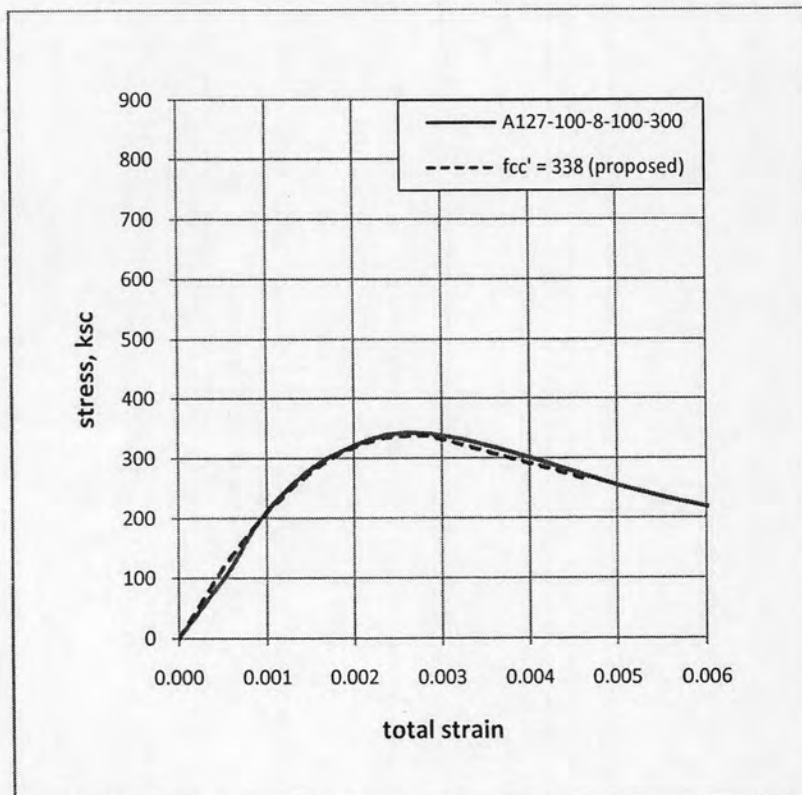


Figure 5.13j Stress – total strain relationship, comparison with the proposed model



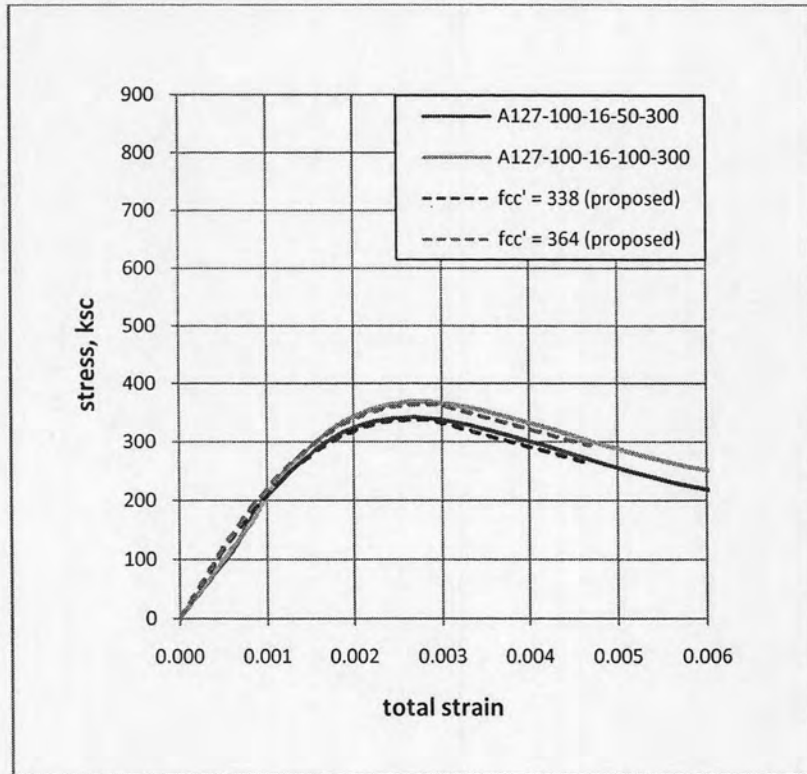


Figure 5.13k Stress – total strain relationship, comparison with the proposed model

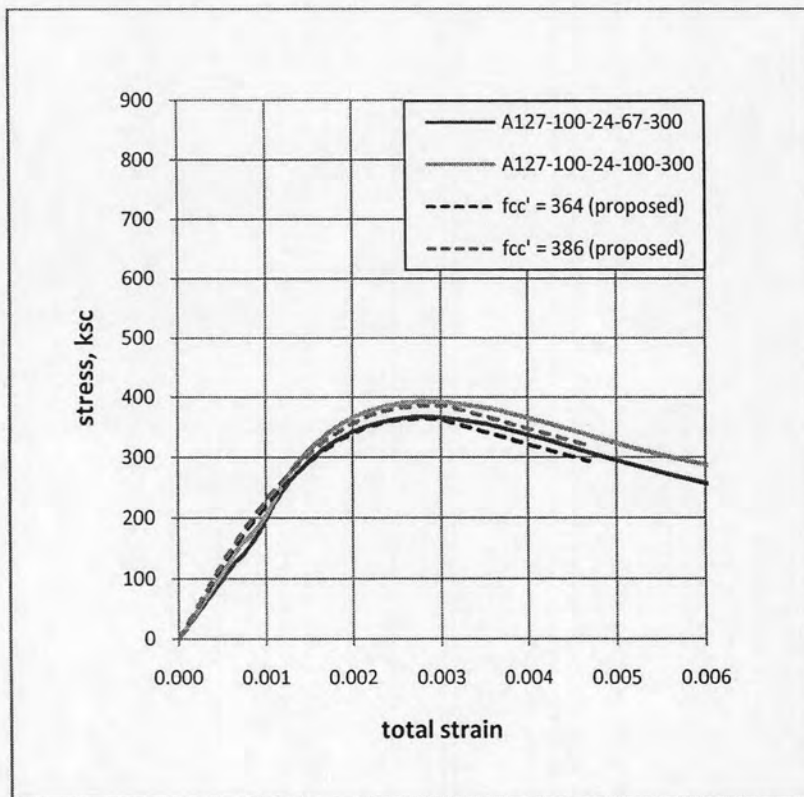


Figure 5.13k Stress – total strain relationship, comparison with the proposed model

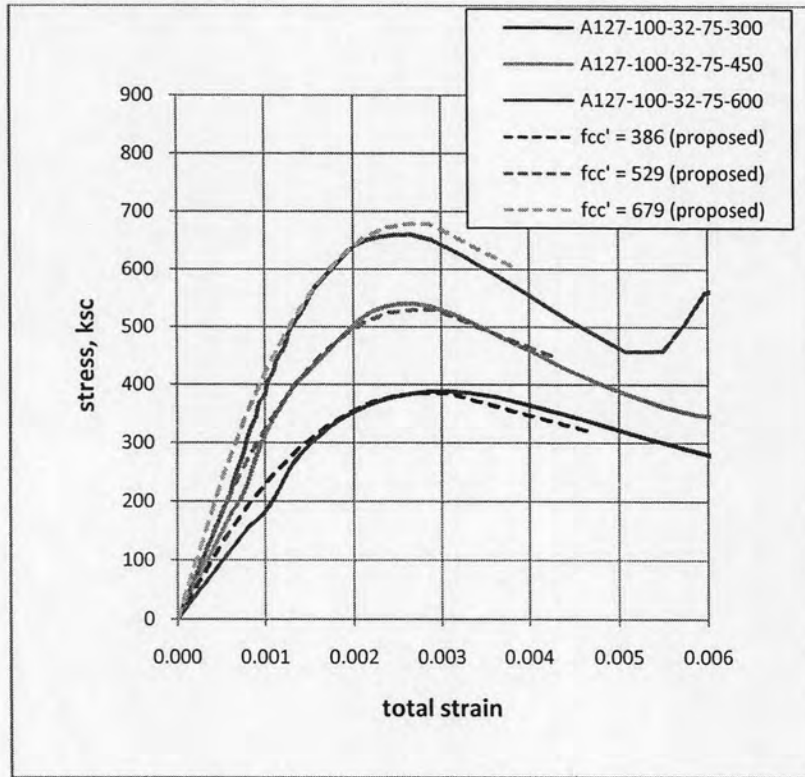


Figure 5.13l Stress – total strain relationship, comparison with the proposed model

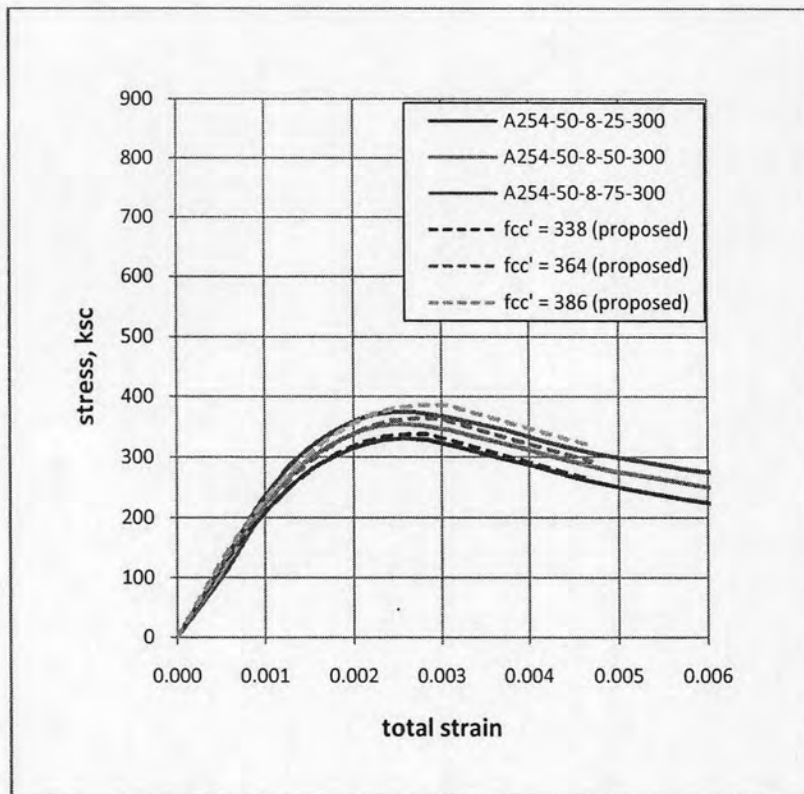


Figure 5.13m Stress – total strain relationship, comparison with the proposed model

The proposed mathematical stress-strain model for axially loaded concrete cylinders with spiral prestressing confinement can simplify and represent complex analytical solution of finite concrete circular cylinder subjected to spiral prestressing confinement.

Applying proposed axially loaded stress-strain model to determine the characteristic of experimental specimens, the results is shown below.

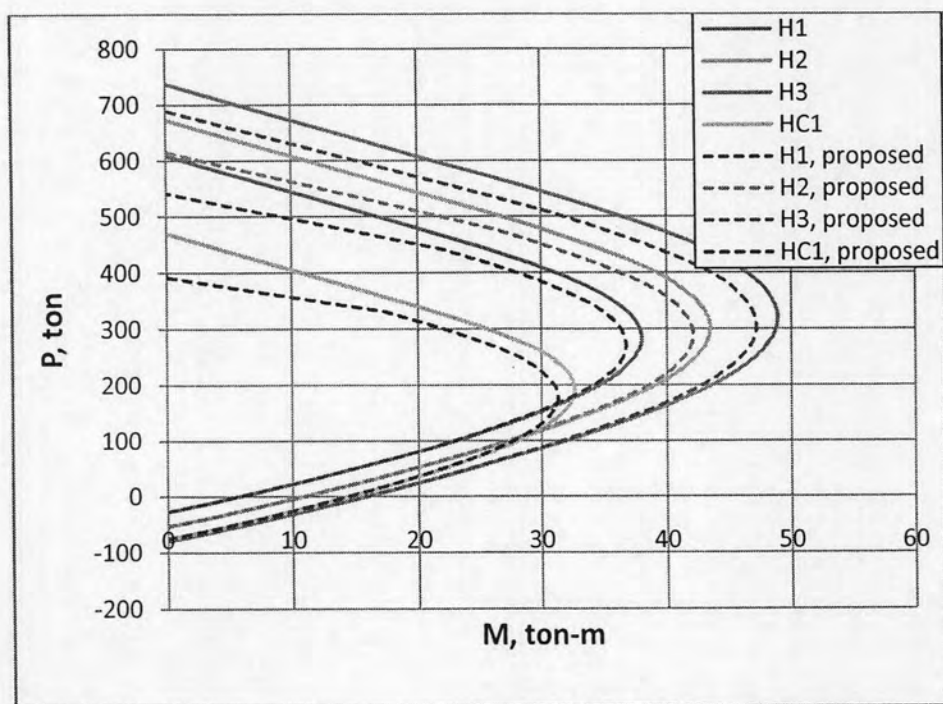


Figure 5.14 P-M diagram of assumed model comparison with proposed model